

Counterdiabatic route for preparation of state with long-range topological order

Sanjeev Kumar , Shekhar Sharma, and Vikram Tripathi

Department of Theoretical Physics, Tata Institute of Fundamental Research, Homi Bhabha Road, Navy Nagar, Mumbai 400005, India



(Received 2 September 2021; revised 1 November 2021; accepted 30 November 2021; published 8 December 2021)

We propose here a counterdiabatic (CD) strategy for the fast preparation of a state with long-range topological order by magnetic field tuning of an initial separable state. For concreteness, we consider the ground state of the honeycomb Kitaev model whose long-range topological order together with the anyonic excitations make it an interesting candidate for fault-tolerant universal quantum computation and storage. We implement an approximate local CD perturbation having the form of the off-diagonal exchange interactions in Kitaev Hamiltonians. The counterdiabatically produced state is found to have a high fidelity ($\gtrsim 0.5$) and retains numerous desired entanglement properties while giving a speed-up of the order of 10^6 . In our study of up to 24-spin clusters we found the fidelity is constrained by the spectral gap rather than the system size.

DOI: [10.1103/PhysRevB.104.245113](https://doi.org/10.1103/PhysRevB.104.245113)

I. INTRODUCTION

The usefulness of a quantum computer depends on the ability to exploit the quantum entanglement and linear superposition absent in their classical counterparts. How well the entanglement property of a quantum many-body state can be utilized in applications depends on the purity of the state, the details of entanglement [1,2], and how feasibly it can be prepared in a short time since long duration preparation protocols may lead to environment-induced decoherence [3–7]. Ideally one should be able to prepare such states from an easily accessible initial quantum state through adiabatic tuning of a suitable Hamiltonian. The quantum adiabatic theorem is a no-go theorem for fast protocols as they would result in nonadiabatic excitations. In systems with a finite gap, shortcuts to adiabaticity (STA) or counterdiabatic (CD) strategies are transitionless driving protocols and a means for quantitatively speeding up the usual adiabatic evolution without compromising the purity of the desired final state [7–10]. CD driving suppresses these nonadiabatic excitations by adding an auxiliary field $\hat{H}_1(t)$ to the system Hamiltonian $\hat{H}_0(t)$. With this auxiliary field, even for a very rapid protocol (as compared to its adiabatic counterpart), the system always traverses the adiabatic manifold of $\hat{H}_0(t)$ and certainly not of $\hat{H}_0(t) + \hat{H}_1(t)$. The explicit expression for the counterdiabatic perturbation [11–13] is given by

$$\hat{H}_1(t) = i\hbar \sum_{m \neq n} \frac{|m\rangle\langle m| \partial_t \hat{H}_0(t) |n\rangle\langle n|}{E_n - E_m}, \quad (1)$$

where $|m\rangle$ denotes the instantaneous eigenstate of $\hat{H}_0(t)$ with eigenvalue E_m . Physically, the CD assistance does not work through increasing the spectral gap (thereby reducing the Landau-Zener transitions) but through a suppression of the matrix elements that would connect the states in the adiabatic manifold to those outside. Expression (1) is reminiscent of

the Berry curvature. Indeed, the transitionless CD driving compensates for the Berry curvature [14] resulting in a higher fidelity at the end of the protocol. The entire spectrum as well as the wave functions of $\hat{H}_0(t)$ are required to construct $\hat{H}_1(t)$. Moreover, the denominators $E_n - E_m$ could vanish, or more generally become exponentially small, in many-body systems. The nonlocality of the CD term and exponential sensitivity to any perturbation in the many-body Hamiltonian [15] is a consequence of constraining the large number of degrees of freedom of the system to the transitionless manifold. This limits the applicability of fast protocols to small few-level systems and the thermodynamic limit is out of question [16]. The perturbation $\hat{H}_1(t)$ suppresses excitations for all $|m\rangle$'s and not just for some special state, for, e.g., a well-separated ground state of the system.

As was pointed out in Ref. [15], a restriction of the exponentially large degrees of freedom in many-body dynamics is not always the goal. Practically, the exact and formal rigidity of Eq. (1) is relaxed by focusing on a specific state only and considering some local operators as an approximation for transitionless driving. Here, we focus on the fast preparation of the ground state of the Kitaev Hamiltonian using the CD protocol. The Kitaev model is an integrable two-dimensional (2D) system of spin-1/2 particles on the honeycomb lattice interacting with peculiar Ising-like direction-dependent local interactions [17]. The model exhibits the spin fractionalization phenomenon with no magnetic order, and elementary excitations consisting of free Majorana fermions and *gapped*, quantized half vortices (visons). Depending on the interaction parameters, the half vortices are Abelian or non-Abelian anyons [17]. For isotropic Kitaev interactions, the Majorana fermions are linearly dispersing and massless, but they become massive above a small characteristic magnetic field. The ground state has long-range topological order [17,18], signified by a finite topological entanglement entropy $\gamma = \ln 2$, which is not destroyed by small magnetic fields. Owing to the nonlocal entanglement and long-range topological order, both

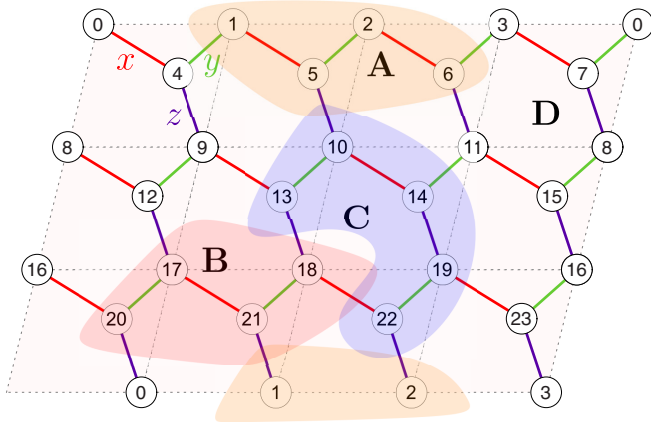


FIG. 1. Schematic of the honeycomb lattice with nearest-neighbor Kitaev interactions described in Eq. (3). Exact diagonalization calculations have been performed with a 24-site cluster with toroidal boundary conditions, and benchmarked with density matrix renormalization group calculations on larger sizes (see Appendix B). For computation of topological entanglement entropy using the Preskill-Kitaev construction (see Sec. III), a partition of a cluster into subsystems $A = \{1, 2, 5, 6\}$, $B = \{17, 18, 20, 21\}$, $C = \{10, 13, 14, 19, 22\}$, and D is shown where D encloses the lattice sites not in A , B , and C .

types of anyons are useful resources for universal quantum computation, providing fault-tolerant quantum memory and quantum gate realization: The Abelian ones are likely to be easily accessible in experiments [19] while the non-Abelian kind is more useful (although less readily realizable) for quantum computation purposes [17].

Even in the presence of a small Zeeman field (smaller than the vison gap), the ground state retains nontrivial topological order [20,21] but opens up a small bulk gap allowing the use of the CD protocol. Cooling down to the ground state is hindered by its complexity: Kitaev states have exponentially small (in

system size) overlaps with low-energy magnons (typically responsible for the thermal relaxation of magnets through spin diffusion to a bath) [20] which are excitations of separable states with magnetic order. A recent study also reveals that long thermalization times are expected in Kitaev systems in the absence of a finite density of visons [22]. The adiabatic preparation of highly entangled quantum states is typically hard to implement owing to the problem of exponentially small (in system size N) spectral gaps near the ground state (see, e.g., Ref. [23]). However, the excitation gap near the ground state of the isotropic Kitaev model vanishes only as $1/\text{poly}[N]$, and, upon the introduction of a magnetic field above a certain small threshold, a finite (Majorana) gap separates its ground state from the rest of the spectrum [17,21], while the vison gap is essentially unchanged. This will be our regime of interest. Since the vison excitations tend to destroy the long-range topological order, the finite vison gap is a desirable feature.

We present a local CD protocol for the high-fidelity preparation of the Kitaev ground state, on timescales significantly shorter than that permitted by the quantum adiabatic theorem. The topological entanglement entropy γ and the (half-vortex) plaquette fluxes W at the end of the protocol are found to be much closer to the equilibrium values compared to that obtained in the same time without the CD protocol. The CD interactions in our model have the form of certain off-diagonal exchange interactions [24–26] in Kitaev systems commonly associated with trigonal deformations. Besides their physical realization in Kitaev materials, such interactions in addition to the Kitaev coupling can be implemented using superconducting quantum circuits [27,28].

The rest of the paper is organized as follows. In Sec. II we introduce our model Hamiltonian and CD protocol. Section III presents our calculations of the state fidelity and other properties such as the topological entanglement entropy and the plaquette flux expectation value. This highlights the difference between our protocol and the naive unassisted protocol in

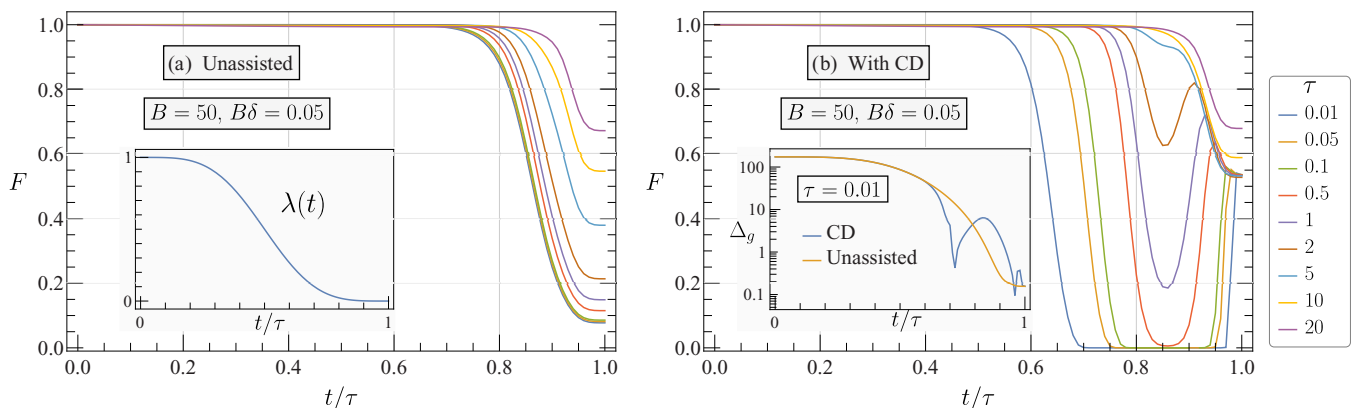


FIG. 2. Plots showing the time evolution of the fidelity $F(t)$ for various duration-of-protocol values τ . In (a) we show the results for the unassisted protocol, i.e., parametric evolution of the Hamiltonian without the CD term, while (b) shows results using the CD assisted protocol. In both cases, we choose an initial large Zeeman field, $B = 50$, which decreases to a small value, $\delta B = 0.05$, at the end of the protocol. Durations varying from $\tau = 0.01$ to $\tau = 20$ are shown, spanning both sides of the validity condition for the adiabatic theorem. For smaller values of τ , CD greatly aids in suppressing the transitions to excited states, resulting in much larger fidelities compared to the unassisted case. For $\tau = 20$, it can be seen that there is no significant difference in the fidelities obtained. The inset in (a) shows the dimensionless smooth ramp $\lambda(t) = \cos^2[\frac{\pi}{2} \sin^2(\frac{\pi t}{27})]$ used in our calculations. The inset in (b) shows the energy gap between the ground state and the first excited state in the two protocols as a function of time t . Clearly, CD does not assist in reducing the minimum energy gap.

the results section. Section IV summarizes our findings and contains a discussion.

II. MODEL AND COUNTERDIABATIC PERTURBATION

In our study, we consider the following Hamiltonian,

$$\hat{H}_0(\lambda) = \hat{H}_k + (\lambda + \delta)\hat{H}_m, \quad (2)$$

where \hat{H}_k the Kitaev Hamiltonian on the honeycomb lattice is given by

$$\hat{H}_k = -J \sum_{\langle ij \rangle_{\gamma\text{-link}}} \sigma_i^{(\gamma)} \sigma_j^{(\gamma)}. \quad (3)$$

Here, i labels the sites and $\langle ij \rangle_{\gamma\text{-link}}$ denotes the nearest neighbors i, j on a link $\gamma = x, y, z$ as shown in Fig. 1. \hat{H}_m corresponds to an external Zeeman field,

$$\hat{H}_m = B \sum_i (\sigma_i^x + \sigma_i^y + \sigma_i^z), \quad (4)$$

and $\lambda(t) \in [0, 1]$ parametrizes the protocol for the Hamiltonian evolution. We set the Kitaev interaction scale $J = 1$. The system is initiated in a high external magnetic field, $B \gg 1$, such that the ground state is a product state, and gapped. The time-dependent part $\lambda(t)$ is a smooth yet fast ramp evolving from 1 to 0 in a time τ , and δ is a small positive constant such that the magnetic field at the end of our protocol is finite, but small, $B\delta \ll 1$. The spectrum remains gapped throughout the parametric evolution (see below), decreasing monotonously as λ decreases.

For a transitionless evolution, we now introduce the CD perturbation to \hat{H}_0 . The CD term of Eq. (1) is expressed through a gauge potential \hat{A}_λ such that $\hat{H}_1(\lambda) = \dot{\lambda}\hat{A}_\lambda$:

$$\hat{H}_{\text{CD}} = \hat{H}_0 + \dot{\lambda}\hat{A}_\lambda. \quad (5)$$

We require the prefactor $\dot{\lambda}$ to vanish at the end points of the protocol; this condition ensures we begin and end in the

ground state manifold of \hat{H}_0 . The gauge potential can be expressed as a sum of nested commutators [29],

$$\hat{A}_\lambda = i \sum_{k=1}^{\infty} \alpha_k \underbrace{[\hat{H}_0, \hat{H}_0, \dots, [\hat{H}_0, \partial_\lambda \hat{H}_0]]}_{2k-1}, \quad (6)$$

where we have suppressed \hbar . The above series expansion gives the exact gauge potential for a gapped system, and higher-order commutators generate increasingly nonlocal contributions. As an approximation, Eq. (6) is truncated after a certain order of expansion $k = l$ to ensure local interactions, while still suppressing excitations to give a reasonable fidelity of a quantum state, which in this paper is set at ≥ 0.5 . The set of variational parameters $\alpha_1, \alpha_2, \dots, \alpha_l$ is determined by minimizing the quantity $S = \langle \hat{G}^2 \rangle - \langle \hat{G} \rangle^2$, where

$$\hat{G} = \partial_\lambda \hat{H}_0 - i[\hat{H}_0, \hat{A}_\lambda], \quad (7)$$

and $\langle \rangle$ denotes averaging with respect to the Boltzmann weight $\exp(-\beta\hat{H}_0)$. The minimization condition ensures transitions due to nonzero off-diagonal elements in the instantaneous Hamiltonian are suppressed [8]. For ease of calculation we focus on the infinite temperature limit ($\beta \rightarrow 0$), where the problem reduces to minimizing $S = \text{Tr}[\hat{G}^2]$. For a detailed derivation, we refer the reader to Ref. [29]. Note the infinite temperature is not ideal for ground state preparation as it treats the excited states on the same footing. We show the CD assistance produces desirable results even in this worst scenario limit. It has been shown that for the one-dimensional Kitaev model, the CD Hamiltonian is of M -body interaction type, thus limiting its practicality [30] for cluster state generation. Limiting ourselves to two-body interactions only, we retain in Eq. (6) only the leading term and obtain (see Appendix A for details)

$$\hat{A}_\lambda^{(1)} = \frac{B/J}{18(\lambda + \delta)^2(B/J)^2 + 10} \left\{ \sum_{\langle ij \rangle_{x\text{-link}}} (\sigma_i^x \sigma_j^y - \sigma_i^x \sigma_j^z) + \sum_{\langle ij \rangle_{y\text{-link}}} (\sigma_i^y \sigma_j^z - \sigma_i^y \sigma_j^x) + \sum_{\langle ij \rangle_{z\text{-link}}} (\sigma_i^z \sigma_j^y - \sigma_i^z \sigma_j^x) + i \leftrightarrow j \right\}. \quad (8)$$

The above gauge potential $\hat{A}_\lambda^{(1)}$ resembles the Γ' interaction in Kitaev systems with the difference that Eq. (8) has asymmetric terms while the Γ' interaction has symmetric ones [24–26], and is associated with trigonal distortions in the lattice. Using Eq. (8) in Eq. (5) gives the CD Hamiltonian which we use in the rest of the paper. Numerical calculations are performed by exact diagonalization of a 24-site cluster (see Fig. 1) using QUSPIN [31,32]. For benchmarking, we compare the energy gap in our system with that of a larger 144-site cluster [obtained via density matrix renormalization group (DMRG)—see Appendix B], and find that the two are in agreement. We thus conclude that the system is gapped throughout the range of magnetic fields we study—this is in contrast with some calculations [33] in the recent literature (based on an apparent power-law decay of ground state spin correlators obtained using DMRG) that claim the existence of

a gapless phase in the range $0.2 \lesssim B \lesssim 0.3$. The finite spectral gap even in the thermodynamic limit is of relevance to our problem since a vanishing gap at intermediate magnetic fields would invalidate the counterdiabatic protocol.

III. RESULTS

Below we show the numerical results for the overlap of the time evolved state, $|\psi[\lambda(t)]\rangle = U(t)|\psi[\lambda(0)]\rangle$, with the ground state $|\phi_{\text{GS}}[\lambda(t)]\rangle$ of the instantaneous Hamiltonian. The fidelity F is defined as $F = |\langle \psi | \phi_{\text{GS}} \rangle|^2$. A smooth ramp with a vanishing time derivative at the end points ensures the initial and final Hamiltonians are the same in the unassisted and CD protocols. For concreteness we choose $\lambda(t) = \cos^2[\frac{\pi}{2} \sin^2(\frac{\pi t}{2\tau})]$ for $t \in [0, \tau]$ as shown in the inset of Fig. 2(a). Figure 2 shows the fidelity of the evolving quantum state in the unassisted [Fig. 2(a)] and CD assisted [Fig. 2(b)]

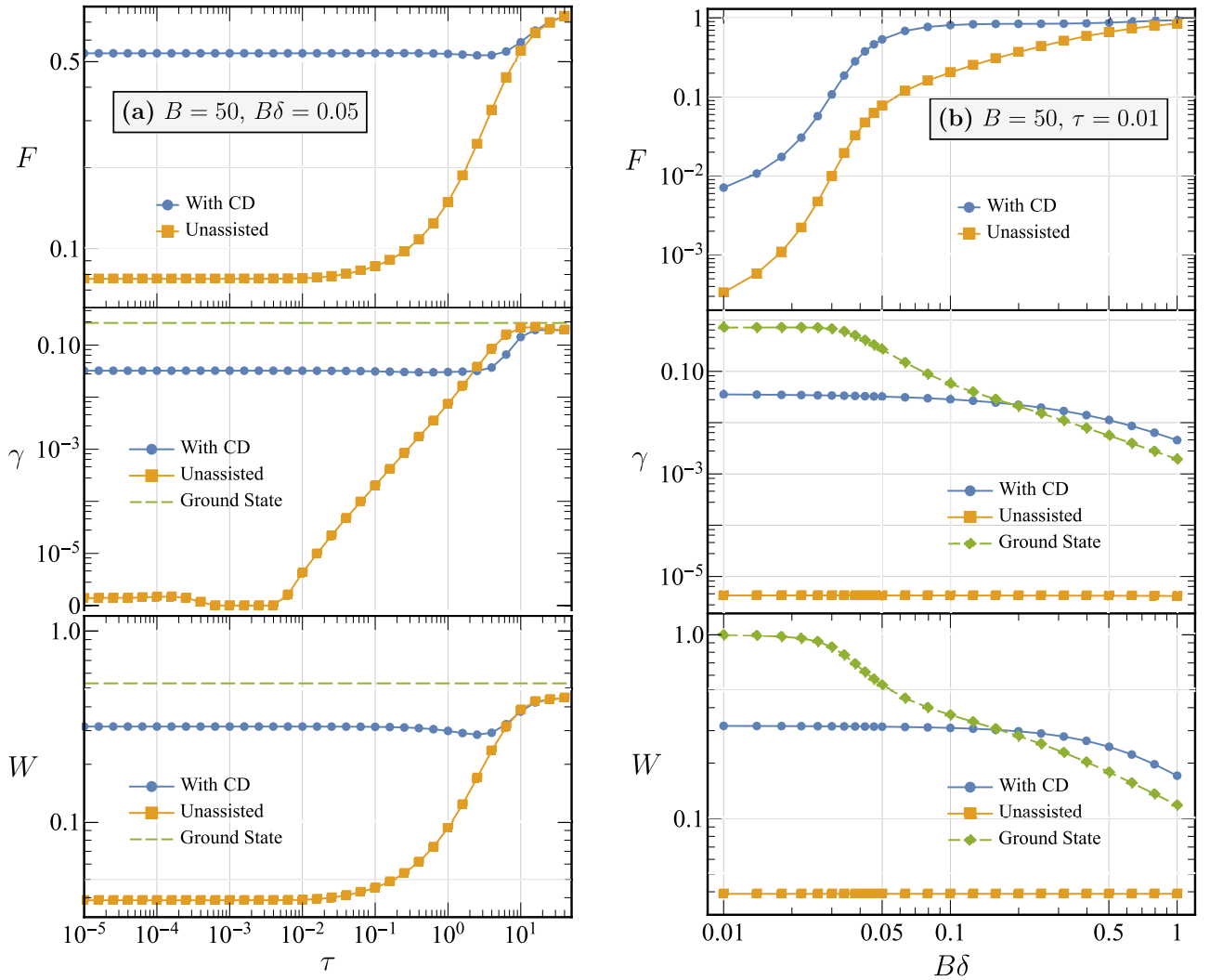


FIG. 3. Plots showing the fidelity (F), entanglement entropy (γ), and expectation value of the \hat{W} (plaquette flux) operator (W) calculated for the quantum state obtained via the CD assisted and the naive, unassisted protocol. In (a) these quantities are shown as a function of a wide range of protocol time duration τ spanning both sides of the validity condition of the adiabatic theorem. The dashed line shows the pure ground state value corresponding to $\delta\hat{H}_m + \hat{H}_k$. The unassisted protocol yields close to zero values for γ and W owing to a lesser fidelity as compared with the CD assisted protocol. γ values smaller than 10^{-6} are suppressed to zero by switching from log scale to linear scale. (b) shows the same quantities as a variation of the final magnetic field in the system $B\delta$. The quantity measures start converging for $\tau = 10$.

protocols for various time durations τ . We note that for $\tau \ll 1$, the fidelity in the CD assisted protocol falls sharply around $t \gtrsim \tau/2$ (even falling to zero for the shorter durations) before jumping to values significantly larger than the unassisted case towards the end of the protocol. The vanishing fidelity during intermediate times is not on account of any closure of the spectral gap [see the inset of Fig. 2(b)] but rather shows that the time evolved state in the CD protocol overlaps poorly with the ground state of the instantaneous Hamiltonian for these intermediate times. However, for $\tau \gg 1$, the two protocols do not show a significant difference. This is in accordance with the fact that for a slow variation of the system parameters, the CD Hamiltonian approaches the adiabatically varying Hamiltonian. From Fig. 2, we see that the fidelity remains approximately unity even for times near the middle of the protocol owing to the still large Zeeman gap. This implies one can start from an initial product state and yet

attain large fidelities for the Kitaev ground state at the end of protocol.

We next compare the usefulness of the quantum state obtained via the two protocols by studying their entanglement entropy and plaquette fluxes. The Kitaev ground state is associated with a finite topological entanglement entropy, which is the part of the von Neumann bipartite entropy, $S_A = \text{Tr} \rho_A \log \rho_A = \alpha L - \gamma$, remaining after subtracting the area law contribution. Here, L is the perimeter of a 2D subsystem A whose bipartite entanglement entropy is S_A . For the Kitaev ground state, $\gamma = \ln 2$. Appropriately choosing four partitions of the lattice (see Fig. 1) and taking a linear combination of entropies of three of the partitions yields γ , which is free from the boundary term [18]:

$$-\gamma = S_A + S_B + S_C - S_{AB} - S_{BC} - S_{AC} + S_{ABC}. \quad (9)$$

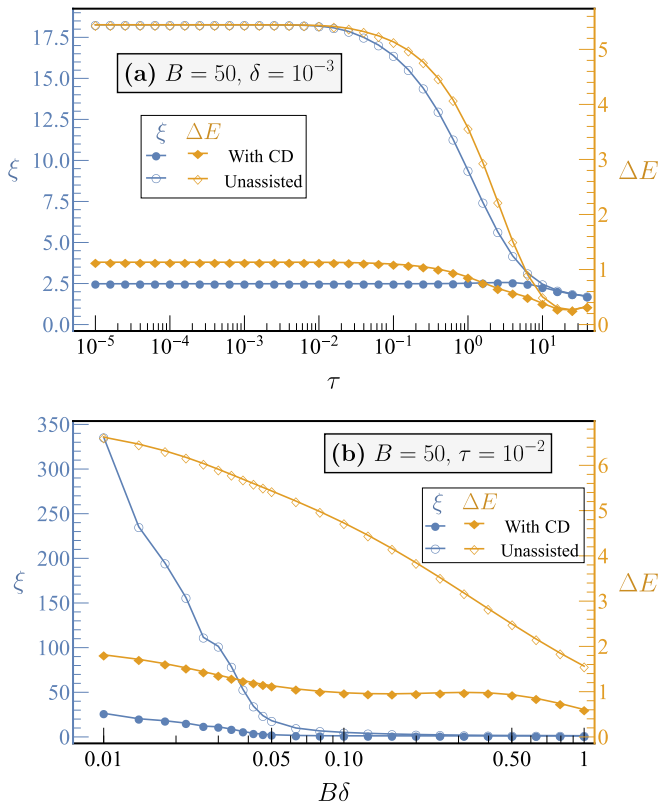


FIG. 4. Support size ξ and change in the energy of the evolved state from the ground state energy $\Delta E = \langle E \rangle - E_{GS}$ are plotted as a function of (a) protocol duration τ and (b) final Zeeman field $B\delta$. In (a) the CD assisted support size, $\xi_{CD} \sim 1$, while for the naive protocol, $\xi \sim 10$, for a wide stretch of τ values. The CD assisted quantum state obtained is localized in the bottom part of the energy spectrum is confirmed by the energy difference ΔE . Again as in Fig. 3(a), the naive driving of Hamiltonian parameters starts coinciding with the transitionless driving at $\tau \sim 10$. Even for very small Zeeman fields, (b) shows the support size ξ_{CD} is still localized to ~ 10 states only in a many-body Hilbert space of dimension 2^{24} while ξ for the unassisted case shows a very rapid variation.

Finite topological entanglement entropy ensures the quantum state is fault tolerant to local disturbances. In addition to the entanglement entropy, the plaquette flux operator \hat{W} is another characteristic quantity in pure Kitaev systems. With reference to Fig. 1, we choose the plaquette $p = \{1, 4, 9, 13, 10, 5\}$ for computing the expectation value of the flux operator defined as $\hat{W}_p = \sigma_1^z \sigma_4^x \sigma_9^y \sigma_{13}^z \sigma_{10}^x \sigma_5^y$. The flux operator commutes with the Kitaev Hamiltonian \hat{H}_k and has eigenvalues $W = \pm 1$. The ground state is characterized by $W = 1$. In Fig. 3 we show the dependence of these quantities on τ [Fig. 3(a)] and the final Zeeman field $B\delta$ [Fig. 3(b)]. The green colored line in Fig. 3 shows the value of these quantities corresponding to the ground state of the final Hamiltonian for comparison. We find that for $\tau \lesssim 1$, the topological entanglement entropy of the quantum state evolved using transitionless driving is an order of magnitude higher than that of the state evolved without it. A finite nonzero γ implies the state is useful for quantum computation. Similarly, the CD assisted protocol yields values of W closer to unity compared to unassisted driving. Because

of better fidelity through the counterdiabatic approach, the final time-evolved quantum state stays close to the true ground state. Quantitatively, this can be expressed in terms of the support size ξ of the quantum state (obtained at the end of the protocol) in the many-body Hilbert space of the exact eigenstates of the final Hamiltonian. The support size ξ is defined as $\xi^{-1} = \sum_i |a_i|^4$, where a_i is the overlap of the quantum state with the many-body eigenstates $|i\rangle$. We observe in Fig. 4(a) support sizes of 2.5 states or less when CD assisted for a wide range of protocol durations while unassisted driving gives support sizes of the order of ten states or more. In the CD protocol, ξ shows a relatively slower variation on changing the final Zeeman field as opposed to the unassisted protocol where ξ rapidly rises for decreasing $B\delta$ as shown in Fig. 4(b). Along with ξ in Fig. 4 we have plotted the energy difference of the obtained quantum state with the pure ground state. We find the energy difference is small for the CD case. We thus claim that the CD aided approach yields the quantum state with high localization (the dimensionality of the many-body Hilbert space for our 24-spin cluster is 2^{24}) near the ground state, with the ground state having the maximum share equal to its fidelity.

IV. DISCUSSION

The Kitaev ground state is useful for universal quantum computing and storage due to its long-range topological order and anyonic excitations. We demonstrated, by using a counterdiabatic strategy, the feasibility of preparing the Kitaev ground state (in the presence of a small Zeeman field sufficient for introducing a bulk spectral gap) with high fidelity on timescales significantly (around 10^6 times) smaller than that permitted by the adiabatic theorem even though the enhancement is still $O(1)$ in a system size as other CD protocols. Although not unique in having a ground state topological order, the Kitaev model works well with the CD protocol because thermalization of this state requires a finite vison density, which is suppressed by the appreciable vison gap in the Kitaev model. Its extreme anisotropic limit, the Kitaev model, reduces to the more well-studied toric code model that also has this topological order. However, because of the very small energies associated with vison excitations in the anisotropic Kitaev model (toric code limit), the topological order is rather fragile [34] unless some way can be found to suppress the visons. Our proposed method relies on limiting the CD expansion to local two-body interactions which makes it practicable for implementation. Despite the local approximation, features such as topological entanglement entropy and nonzero flux expectation were shown to be preserved much better than unassisted protocols in the same time duration. To further increase the fidelity and other topological features it is necessary to include higher-order (and more nonlocal) terms neglected in our approximate CD protocol. Our calculations have been performed on 24-spin clusters, and it is not *a priori* evident how the neglected nonlocal CD terms will affect the fidelity for larger system sizes. Nevertheless we do have some understanding of the trend. In the Appendix B we show the fidelities attained for three different system sizes $N = 12, 18, 24$. We observed that comparable (and even

better) fidelities are obtained with increasing system size with our CD protocol. Together with Fig. 3(b), this suggests the fidelity is limited much more by the size of the spectral gap than the size of the system. Further studies should improve our understanding of the scaling of fidelity with larger system sizes.

ACKNOWLEDGMENT

We thank Aman Kumar for sharing the DMRG result of energy gaps.

APPENDIX A: GAUGE POTENTIAL \hat{A}_λ

We sketch the steps involved to obtain the counterdiabatic perturbation to the Hamiltonian \hat{H}_0 . For a two-body local interaction, we expand Eq. (6) to leading order:

$$\hat{A}_\lambda^{(1)} = i\alpha_1[\hat{H}_0, \partial_\lambda \hat{H}_0] = i\alpha_1[\hat{H}_k, \hat{H}_m]. \quad (\text{A1})$$

Let the Zeeman field coupling constant $\mathbf{B} = (B_x, B_y, B_z)$. In our analysis, we considered the field along the [111] direction with $B_x = B_y = B_z = B$. The commutator in Eq. (8) can be

written as a sum of three terms $[\hat{H}_k, \hat{H}_m] = \hat{\mathcal{X}} + \hat{\mathcal{Y}} + \hat{\mathcal{Z}}$ which are given by

$$\hat{\mathcal{X}} = 2iB_x J \left\{ \sum_{\langle jk \rangle_{z\text{-link}}} (\sigma_j^y \sigma_k^z + \sigma_j^z \sigma_k^y) - \sum_{\langle jk \rangle_{y\text{-link}}} (\sigma_j^y \sigma_k^z + \sigma_j^z \sigma_k^y) \right\}, \quad (\text{A2})$$

$$\hat{\mathcal{Y}} = 2iB_y J \left\{ \sum_{\langle jk \rangle_{x\text{-link}}} (\sigma_j^z \sigma_k^x + \sigma_j^x \sigma_k^z) - \sum_{\langle jk \rangle_{z\text{-link}}} (\sigma_j^z \sigma_k^x + \sigma_j^x \sigma_k^z) \right\}, \quad (\text{A3})$$

$$\hat{\mathcal{Z}} = 2iB_z J \left\{ \sum_{\langle jk \rangle_{y\text{-link}}} (\sigma_j^x \sigma_k^y + \sigma_j^y \sigma_k^x) - \sum_{\langle jk \rangle_{x\text{-link}}} (\sigma_j^x \sigma_k^y + \sigma_j^y \sigma_k^x) \right\}. \quad (\text{A4})$$

The variational parameter α_1 is found by constructing the operator \hat{G} as defined in Eq. (7) and minimizing $S = \text{Tr} \hat{G}^2$. The leading order of \hat{G} can be expressed as

$$\begin{aligned} \hat{G}^{(1)} &= \partial_\lambda \hat{H}_0 - i[\hat{H}_0, \hat{A}_\lambda^{(1)}] \\ &= \hat{H}_m - \alpha_1(\lambda + \delta)[\hat{H}_m, [\hat{H}_m, \hat{H}_k]] - \alpha_1[\hat{H}_k, [\hat{H}_m, \hat{H}_k]]. \end{aligned} \quad (\text{A5})$$

The minimization condition $\delta S / \delta \alpha_1 = 0$ yields

$$\alpha_1 = \frac{(\lambda + \delta)\text{Tr}(\hat{H}_m[\hat{H}_m, [\hat{H}_m, \hat{H}_k]]) + \text{Tr}(\hat{H}_m[\hat{H}_k, [\hat{H}_m, \hat{H}_k]])}{(\lambda + \delta)^2\text{Tr}([\hat{H}_m, [\hat{H}_m, \hat{H}_k]])^2 + \text{Tr}([\hat{H}_k, [\hat{H}_m, \hat{H}_k]])^2 + 2(\lambda + \delta)\text{Tr}([\hat{H}_m, [\hat{H}_m, \hat{H}_k]][\hat{H}_k, [\hat{H}_m, \hat{H}_k]])}. \quad (\text{A6})$$

The traces are evaluated numerically resulting in

$$\alpha_1 = \frac{-1/4}{9(\lambda + \delta)^2 B^2 + 5J^2}. \quad (\text{A7})$$

Substituting α_1 in Eq. (A1) gives the gauge potential $\hat{A}_\lambda^{(1)}$.

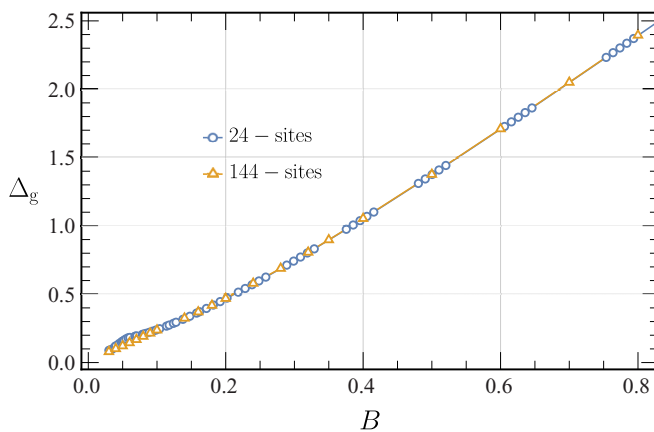


FIG. 5. Ground state energy gap for the Hamiltonian $\hat{H} = \hat{H}_m + \hat{H}_k$ as calculated for 24 sites using exact diagonalization and 144 sites via DMRG as a function of Zeeman field coupling B is shown. The two cases coincide for a wide range of magnetic field values encountered in the naive as well as CD assisted protocol [see the inset of Fig. 2(b)].

APPENDIX B: ENERGY GAP AND FINITE SIZE DEPENDENCE OF FIDELITY

Higher fidelities in CD assisted protocols are aided by the mass gap present in the Kitaev system in the presence of a Zeeman field. Here, we illustrate this gap is not a finite size effect. Figure 5 shows the comparison of the energy

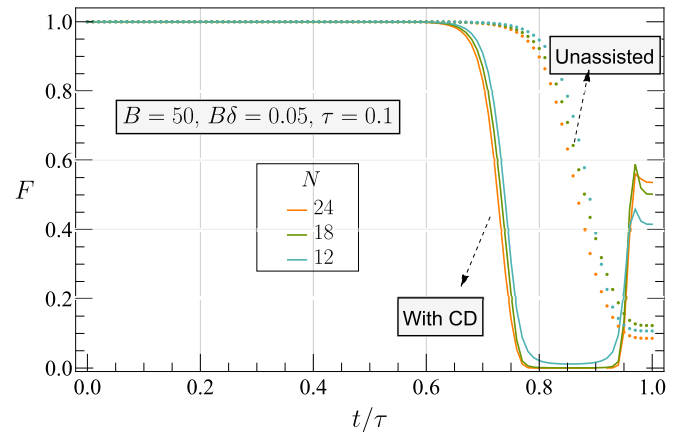


FIG. 6. Fidelities obtained for three different system sizes up to $N = 24$ are shown. Solid lines depict the CD assisted protocol while the dotted lines correspond to the unassisted protocol. The fidelity shows an increasing trend with system size, suggesting that in our model it is limited primarily by the size of the spectral gap (finite even in the thermodynamic limit) and less so by the system size.

gap between the ground state and first excited state for the Hamiltonian $\hat{H} = \hat{H}_m + \hat{H}_k$ in 24-site and 144-site lattices. All 24-site calculations are performed via exact diagonalization in QUSPIN while the larger 144-site energy gap calculation is done using the finite size DMRG. We note the gap coincides

for the two cases for a wide range of magnetic fields encountered in the protocol [see the inset of Fig. 2(b)].

In Fig. 6 we show the dependence of the fidelity on the system size of up to 24-spin clusters. We see the fidelities are comparable (and even better) for the increasing system sizes.

-
- [1] A. Y. Kitaev, *Ann. Phys.* **303**, 2 (2003).
- [2] D. Gross, S. T. Flammia, and J. Eisert, *Phys. Rev. Lett.* **102**, 190501 (2009).
- [3] S. He, S.-L. Su, D.-Y. Wang, W.-M. Sun, C.-H. Bai, A.-D. Zhu, H.-F. Wang, and S. Zhang, *Sci. Rep.* **6**, 1 (2016).
- [4] S. Bandyopadhyay and A. Dutta, *Phys. Rev. B* **102**, 094301 (2020).
- [5] A. Hama and D. A. Lidar, *Phys. Rev. Lett.* **100**, 030502 (2008).
- [6] A. C. Santos and M. S. Sarandy, *J. Phys. A: Math. Theor.* **51**, 025301 (2017).
- [7] D. Guéry-Odelin, A. Ruschhaupt, A. Kiely, E. Torrontegui, S. Martínez-Garaot, and J. G. Muga, *Rev. Mod. Phys.* **91**, 045001 (2019).
- [8] M. Kolodrubetz, D. Sels, P. Mehta, and A. Polkovnikov, *Phys. Rep.* **697**, 1 (2017).
- [9] X. Chen, A. Ruschhaupt, S. Schmidt, A. del Campo, D. Guéry-Odelin, and J. G. Muga, *Phys. Rev. Lett.* **104**, 063002 (2010).
- [10] S. Deffner, C. Jarzynski, and A. del Campo, *Phys. Rev. X* **4**, 021013 (2014).
- [11] C. Jarzynski, *Phys. Rev. A* **88**, 040101(R) (2013).
- [12] M. V. Berry, *J. Phys. A: Math. Theor.* **42**, 365303 (2009).
- [13] C. W. Duncan and A. Del Campo, *New J. Phys.* **20**, 085003 (2018).
- [14] A. Hartmann and W. Lechner, *New J. Phys.* **21**, 043025 (2019).
- [15] D. Sels and A. Polkovnikov, *Proc. Natl. Acad. Sci. USA* **114**, E3909 (2017).
- [16] E. J. Meier, K. Ngan, D. Sels, and B. Gadway, *Phys. Rev. Research* **2**, 043201 (2020).
- [17] A. Kitaev, *Ann. Phys.* **321**, 2 (2006).
- [18] A. Kitaev and J. Preskill, *Phys. Rev. Lett.* **96**, 110404 (2006).
- [19] S. Lloyd, *Quantum Inf. Process.* **1**, 13 (2002).
- [20] A. Kumar and V. Tripathi, *Phys. Rev. B* **102**, 100401(R) (2020).
- [21] M. Gohlke, R. Moessner, and F. Pollmann, *Phys. Rev. B* **98**, 014418 (2018).
- [22] I. C. Fulga, M. Maksymenko, M. T. Rieder, N. H. Lindner, and E. Berg, *Phys. Rev. B* **99**, 235408 (2019).
- [23] B. Altshuler, H. Krovi, and J. Roland, *Proc. Natl. Acad. Sci. USA* **107**, 12446 (2010).
- [24] S. D. Das, S. Kundu, Z. Zhu, E. Mun, R. D. McDonald, G. Li, L. Balicas, A. McCollam, G. Cao, J. G. Rau, H.-Y. Kee, V. Tripathi and S. E. Sebastian, *Phys. Rev. B* **99**, 081101(R) (2019).
- [25] D. Takikawa and S. Fujimoto, *Phys. Rev. B* **102**, 174414 (2020).
- [26] D. Takikawa and S. Fujimoto, *Phys. Rev. B* **99**, 224409 (2019).
- [27] M. Sameti and M. J. Hartmann, *Phys. Rev. A* **99**, 012333 (2019).
- [28] J. Q. You, X.-F. Shi, X. Hu, and F. Nori, *Phys. Rev. B* **81**, 014505 (2010).
- [29] P. W. Claeys, M. Pandey, D. Sels, and A. Polkovnikov, *Phys. Rev. Lett.* **123**, 090602 (2019).
- [30] T. H. Kyaw and L.-C. Kwek, *New J. Phys.* **20**, 045007 (2018).
- [31] P. Weinberg and M. Bukov, *SciPost Phys.* **2**, 003 (2017).
- [32] P. Weinberg and M. Bukov, *SciPost Phys.* **7**, 20 (2019).
- [33] N. D. Patel and N. Trivedi, *Proc. Natl. Acad. Sci. USA* **116**, 12199 (2019).
- [34] T.-C. Lu, T. H. Hsieh, and T. Grover, *Phys. Rev. Lett.* **125**, 116801 (2020).